ACS OMEGA

http://pubs.acs.org/journal/acsodf

Article

Aptamer Sandwich Assay for the Detection of SARS-CoV-2 Spike Protein Antigen

Marketa Svobodova,[○] Vasso Skouridou,[○] Miriam Jauset-Rubio, Irene Viéitez, Alberto Fernández-Villar, Jorge Julio Cabrera Alvargonzalez, Eva Poveda, Clara Benavent Bofill, Teresa Sans, Abdulaziz Bashammakh, Abdulrahman O. Alyoubi, and Ciara K. O'Sullivan*

Cite This: *ACS Omega* 2021, 6, 35657−35666

Read Online

ACCESS | Metrics & More | Article Recommendations | Supporting Information

ABSTRACT: The novel severe acute respiratory syndrome coronavirus (SARS-CoV-2) emerged at the end of 2019, resulting in the ongoing COVID-19 pandemic. The high transmissibility of the virus and the substantial number of asymptomatic individuals have led to an exponential rise in infections worldwide, urgently requiring global containment strategies. Reverse transcription-polymerase chain reaction is the gold standard for the detection of SARS-CoV-2 infections. Antigen tests, targeting the spike (S) or nucleocapsid (N) viral proteins, are considered as complementary tools. Despite their shortcomings in terms of sensitivity and specificity, antigen tests could be deployed for the detection of potentially contagious individuals with high viral loads. In this work, we sought to develop a sandwich aptamer-based assay for the detection of the S protein of SARS-CoV-2. A detailed study on the binding properties of aptamers to the receptor-binding domain of the S protein in search of aptamer pairs forming a sandwich is presented. Screening of aptamer pairs and optimization of assay conditions led to the development of a laboratory-based sandwich assay able to detect 21 ng/mL (270 pM) of the protein with negligible cross-reactivity with the other known human coronaviruses. The detection of 375 pg of the protein in viral transport medium demonstrates the compatibility of the assay with clinical specimens. Finally, successful detection of the S antigen in nasopharyngeal swab samples collected from suspected patients further establishes the suitability of the assay for screening purposes as a complementary tool to assist in the control of the pandemic.

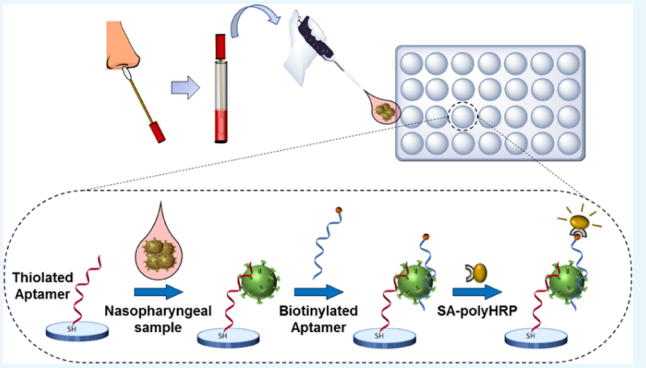

INTRODUCTION

Coronaviruses (CoV's) are a group of highly diverse, enveloped, single-stranded, and positive-sense RNA viruses which cause diseases involving respiratory, enteric, hepatic, and neurological systems with a high range of severity among humans and animals.[1,2] To date, there are seven documented human CoV's (HCoV's). These include HCoV-NL63, HCoV-HKU1, HCoV-OC43, and HCoV-229E, which cause asymptomatic or mild respiratory infections. Severe acute respiratory syndrome (SARS)-CoV (SARS-CoV) and middle east respiratory syndrome (MERS)-CoV (MERS-CoV), on the other hand, are highly pathogenic and lethal HCoV's.[3] The most recently recorded pathogenic HCoV is the novel SARS-CoV-2, previously named 2019-nCoV, which is the causative agent of the respiratory illness COVID-19, leading to millions of deaths around the world.[4,5]

SARS-CoV-2 contains four major structural proteins: the spike (S), envelope (E), membrane (M), and nucleocapsid (N) proteins.[6−8] S, E, and M are anchored on the viral surface envelope, whereas N is found inside the virion. Protein S is a typical class I fusion glycoprotein that undergoes proteolytic cleavage, resulting in two subunits S1 and S2. The receptor-binding domain (RBD) is part of the S1 subunit and it binds to a host receptor angiotensin-converting enzyme II (ACE2) on cells and then fuses the viral and host membranes through the S2 subunit.[9−11] The fundamental role of S protein in viral attachment, fusion, and entry to the cells renders it a key target for the diagnosis and treatment of SARS-CoV-2,[12] and it has indeed been the main protein target used in currently approved COVID-19 vaccines.[13]

The current COVID-19 diagnostic products can be grouped into serological and diagnostic tests.[14] Serological tests measure antibodies against SARS-CoV-2 in patients to test who may still be at risk and more broadly assess the prevalence of COVID-19 in a population. Diagnostic tests focus on

Received: October 7, 2021
Accepted: November 25, 2021
Published: December 15, 2021

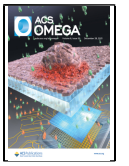

nucleic acid or viral antigen detection. The standards for the diagnosis of COVID-19 are nucleic acid amplification tests (NAATs), including reverse transcription-polymerase chain reaction (RT-PCR),[15] transcription-mediated amplification (TMA), and loop-mediated isothermal amplification (LAMP). For the specific detection of SARS-CoV-2, diagnostic panels consisting of primers specific to SARS-CoV-2 are used and provide results in 2−3 h. Most of the available NAATs utilize primers selected from N, E, and S proteins and open reading frame 1 ab (ORF1ab) genes.[16,17] NAAT-based point-of-care (POC) tests are already available in the market offering easier handling and shorter turnaround times but still need to be used in physician offices or clinics. Moreover, molecular tests are expensive and cannot cover the massive testing needs for the control of the pandemic situation. Limited availability of NAAT testing capacity has hindered response effort even in well-funded health-care systems, while in low- and middle-income countries, the situation is even more complicated. Therefore, it is critical to develop alternative tests not limited to testing at large centralized facilities.

Antigen tests detect the presence or absence of the viral proteins (antigens) and offer an inexpensive solution for population-scale screening of SARS-CoV-2, particularly with lateral flow rapid tests. Currently, several rapid antigen tests are available in the market having received an emergency use authorization (EUA) from the United States Food and Drug Administration (FDA).[17−20] The majority of these tests are based on the detection of the N protein antigen. A recent study suggested the combined detection of the two antigens for more reliable results based on their finding that an S-based assay was more specific, whereas an N-based one was more sensitive for the detection of SARS-CoV-2 infections.[21] Due to the advantages they present compared to RT-PCR, rapid antigen tests could even substitute NAAT-based testing for screening purposes. Several studies demonstrated a high correlation between the antigen concentration and the viral load, especially in clinical samples with low cycle threshold (Ct) values corresponding to samples with a high viral load.[22−24] It has been reported that the concentration of the N protein antigen in symptomatic patient samples taken within 7 days of symptom onset correlates better with virus culture-based detection of the infectious virus than Ct values,[25] and thus, antigen tests can be used to screen for infectious individuals.[25] However, antigen tests with low sensitivity can produce false negative results for samples with a low viral load (high Ct values).[26,27]

Sandwich-type immunoassays have been established in the field of viral diagnostics for the detection and quantification of viral antigens, with their inherent characteristics of superior sensitivity and specificity, greatly reducing false-positive results. Taking lessons from the first SARS-CoV outbreak for which extremely sensitive sandwich ELISA assays targeting the nucleoprotein of the virus were developed, achieving detection limits of 50 pg/mL,[28] the first immunoassays developed for the detection of SARS-CoV-2 antigens were also based on the N protein.[29,30] In parallel, a variety of immunoassays and immunosensors,[31−37] ACE2 receptor-based biosensor,[37,38] or even glycan-based lateral flow assay[39] have also been reported in the literature for the detection of the S antigen, achieving limits of detection (LODs) from 1 fg/mL to 5 μg/mL.

Aptamers are considered as an alternative to antibodies and can be potentially used to improve currently available detection methods. Aptamers are synthetic nucleic acids selected via systematic evolution of ligands by exponential enrichment (SELEX),[40−42] forming three-dimensional structures allowing them to specifically bind to any kind of target molecules. They are inexpensive, stable, and versatile and can be easily modified and applied to virtually any kind of assay. The vast majority of aptamer selection strategies focus on obtaining at least one aptamer with high affinity and specificity, and there are a limited number of reports detailing aptamer-based sandwich assays.[43−45]

Recently, aptamers have been selected against the RBD of SARS-CoV-2 spike glycoprotein.[46] Two high binding affinity sequences were identified, aptamer 1 and 4, with affinity dissociation constant values (K_D) of 3.1 and 13 nM, respectively. Truncated versions of these aptamers (aptamer 1C, 51 nt and aptamer 4C, 67 nt) were shown to maintain their high affinity with only slightly lower K_D values of 5.8 and 19.9 nM for 1C and 4C, respectively. Aptamer 1C was later used for the development of a surface-enhanced Raman spectrometry (SERS)-based aptasensor for the detection of sub-picomolar concentrations of the spike protein,[47] while aptamer 4C immobilized on gold nanostars was exploited for spike protein detection using distance-dependent nanoparticle surface energy transfer (NSET) spectroscopy, achieving an LOD of 1.7 fM.[48] Other high affinity spike protein-binding aptamers (K_D in the low nanomolar range) have also been reported,[49−53] and in silico modeling has also been used to predict aptamers for binding the spike protein.[54−56]

Overall, these are the only studies reported to date regarding the development of S antigen-binding aptamers and the respective applications developed for the detection of SARS-CoV-2 infections.

The aim of this work was to develop an aptamer-based sandwich assay for the detection of the S antigen of SARS-CoV-2. We envisioned that once a microplate sandwich assay was established, its format could potentially be transferred to a POC-compatible format such as a lateral flow assay. To this end, all aptamer candidates previously reported,[46] six full-length and two shortened aptamer versions, were used in combinatorial experiments in order to identify pairs of aptamers able to detect the S1 antigen protein of SARS-CoV-2. Direct enzyme-linked aptamer assays (direct ELAAs) were initially performed to evaluate the affinity and specificity of the eight aptamers, followed by screening of different combinations of aptamers in the sandwich format to identify the best-performing aptamer pair in terms of sensitivity and specificity. Finally, a sandwich ELAA was developed using the best aptamer pair (Figure 1) and used for the detection of the spike antigen of SARS-CoV-2 in nasopharyngeal (NP) swab samples from COVID-19 patients.

RESULTS AND DISCUSSION

Affinity and Specificity of the Aptamers. With the COVID-19 pandemic caused by the SARS-CoV-2 virus still advancing more than a year since its outbreak and the global vaccination rates not reaching the desired level for achieving herd immunity, availability of SARS-CoV-2 diagnostic tools to implement the current monitoring and containment strategies is essential. Antigen tests have emerged as complementary tools to RT-PCR and typically detect the S or N viral proteins. The lower homology of S proteins among the known HCoV's compared to the N protein renders the S protein as the most appropriate antigen for the development of sensitive and specific antigen tests. Viral antigen tests have recently emerged

https://doi.org/10.1021/acsomega.1c05521
ACS Omega 2021, 6, 35657−35666

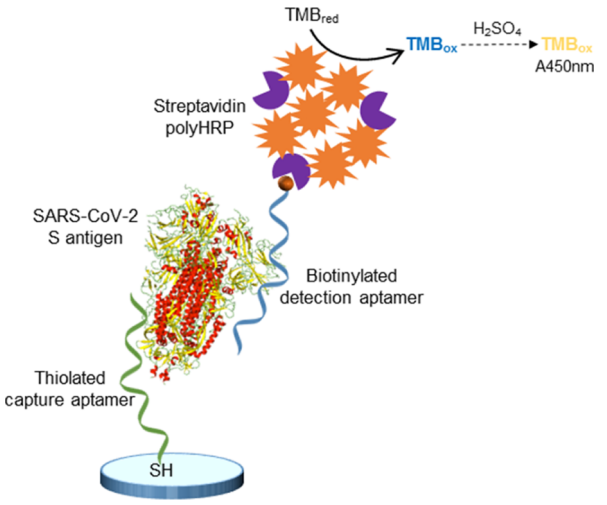

Figure 1. Detection of the SARS-CoV-2 S antigen with the aptamer sandwich assay.

as key diagnostic tools that can implement the global efforts of monitoring and containment of the COVID-19 pandemic.[57] With the aim of developing an antigen test for SARS-CoV-2 based on the spike glycoprotein, previously reported spike protein RBD domain-binding aptamers[46] were exploited. The binding affinities of all full-length aptamers (1−6) and the two truncated versions (1C and 4C) for both S1 and RBD proteins of SARS-CoV-2 were initially evaluated using direct ELAAs. The K_D values calculated for each aptamer and both proteins are shown in Table 1, while the binding curves can be found in

Table 1. Affinity of the Aptamers for S1 and RBD SARS-CoV-2 S Protein Domains

	S1		RBD	
	K_D (nM)	R^2	K_D (nM)	R^2
Apt1	10.2 ± 2.7	0.9875	39.0 ± 11.2	0.9903
Apt2	0.2 ± 0.1	0.9768	7.7 ± 1.4	0.9887
Apt3	5.3 ± 0.5	0.9976	10.9 ± 2.9	0.9706
Apt4	3.3 ± 0.7	0.9869	34.6 ± 17.8	0.9851
Apt5	11.3 ± 6.1	0.9810	29.8 ± 17.8	0.9713
Apt6	3.4 ± 1.1	0.9879	32.2 ± 7.3	0.9701
Apt1C	8.1 ± 1.0	0.9939	21.0 ± 2.7	0.9916
Apt4C	11.1 ± 2.7	0.9623	20.8 ± 5.4	0.9792

Figure S1 (Supporting Information). All the K_D values were observed to be in the low nanomolar range, demonstrating the high affinity of the aptamers. Slightly different K_D values of aptamers 1 and 4 and their shortened versions 1C and 4C for the RBD compared to previously published results can be attributed to the different binding assays employed and the aptamer modifications. In the original report,[46] site-directed immobilization of the RBD protein on nickel beads was achieved via its his-tag, whereas random orientation is expected when the protein is adsorbed directly on a microtiter plate for the ELAAs. Moreover, the type of chemical modification added to the aptamer sequence could affect aptamer folding and therefore its binding properties. For all studied aptamers, higher affinities to S1 as compared to the RBD were observed. It is possible that the conformation of the S1 protein, which is larger compared to the RBD (76.5 kDa vs 26.5 kDa), is different after physical adsorption to the microtiter plate and could provide improved accessibility of the aptamer to the binding site on the RBD. Another factor that could contribute to these differences is the variability of the quality of the recombinant proteins and the organisms used for their expression. Similar results of higher affinity to S1 compared to the RBD were also reported for peptide binders selected recently against SARS-Cov-2 spike protein.[58]

The specificity of an assay is a critical factor determining its analytical performance, particularly when screening for SARS-CoV-2 antigens. The potential cross-reactivity of the aptamers being evaluated in this work for the development of a SARS-CoV-2 antigen test with other HCoV's was thus investigated, considering that the genome of SARS-CoV-2 shares 65−82.5% sequence homology with the other known HCoV's such as HCoV-HKU1, HCoV-NL63, HCoV-229E, HCoV-OC43, SARS-CoV, and MERS-CoV.[59] As commented previously, the target protein of the SARS-CoV-2 antigen test is the spike glycoprotein of SARS-CoV-2. Taking into account that the protein in its prefusion state is assembled on the virion envelope by the S1 and S2 domains after proteolysis, as well as the limited commercial availability of recombinant RBD protein domains from the different HCoV strains, S1 was chosen as the most appropriate protein to be used from this point on. Hence, the binding of the aptamers to the S1 subunit of the other HCoV's was evaluated by a direct ELAA (Figure 2). The lowest cross-reactivity to other HCoV's was exhibited

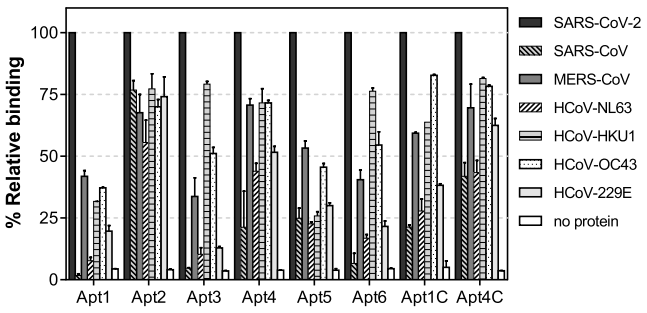

Figure 2. Specificity of the aptamers evaluated by direct ELAA. The relative binding of each aptamer was calculated using constant concentrations of aptamers (200 nM) and S1 proteins from the different HCoV's (2 μg/mL). The error bars correspond to the standard deviation from duplicate measurements.

by aptamers Apt1 and Apt5. Apt1 appeared to be the most selective among the aptamers studied and it showed less than 20% relative binding to HCoV-NL63 and HCoV-229E. These are alpha CoV's, and the RBD from SARS-CoV-2, which is a beta CoV, shares only 20% sequence homology.[60] Spike proteins from strains of the beta CoV genus, including MERS-CoV, HCoV-OC43, and HCov-HKU1, share higher sequence and structural similarities.[61] Apt1 showed cross-reactivity with S1 from these viruses (20−42% relative binding), suggesting that a similar binding site might be recognized. Surprisingly, no binding of Apt1 was detected to S1 from SARS-CoV which is the most recent common ancestor of SARS-CoV-2[62] and with which it shares a 74% sequence identity within the RBD region.[63] The specificity of Apt5 followed a similar pattern with Apt1. The rest of the aptamers, however, showed higher cross-reactivity with the other CoV's. Moreover, decreased specificity was observed for the truncated aptamers Apt1C and Apt4C as compared to their full-length counterparts despite maintaining their high affinity.

https://doi.org/10.1021/acsomega.1c05521
ACS Omega 2021, 6, 35657−35666

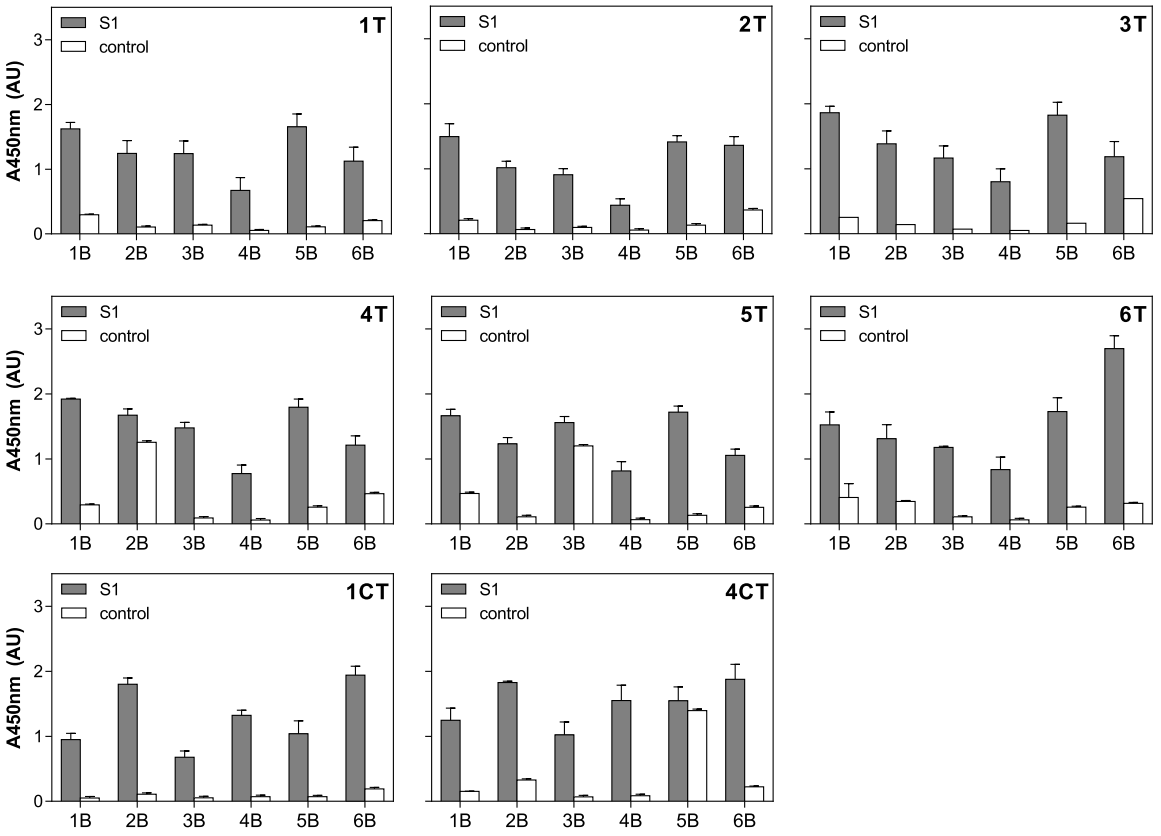

Figure 3. Screening of aptamer pairs for the detection of SARS-CoV-2 S1 protein. Each thiolated capture aptamer (Apt**x**T) was analyzed in combination with each of the biotinylated reporter aptamers (Apt**x**B) using a constant concentration of S1. No protein was added for the control samples. The number refers to the number of the aptamer tested, T indicates the thiolated aptamer and B indicates the biotinylated aptamer.

Screening of Aptamer Pairs. The advantage of sandwich-type aptamer-based assays is that the combination of two aptamers can considerably improve the specificity and sensitivity of the assay. In order to find the most appropriate pair of aptamers for the development of the SARS-CoV-2 antigen test, pairwise experiments combining all eight aptamer candidates were carried out. Thiolated capture aptamers (1T–6T, 1CT, and 4CT) and biotinylated reporter aptamers (1B–6B) were thus combined in a sandwich format (Figure 1) using constant concentrations, and the results are shown in Figure 3. Nonspecific interactions between capture and reporter aptamers in the absence of protein were also evaluated. The majority of combinations tested resulted in the successful detection of S1 in a sandwich format, indicating that capture and reporter aptamers potentially bind to different binding sites on the target protein. Signals observed in the absence of S1 protein with the aptamer combinations of 4T with 2B, 5T with 3B, and 4CT with 5B could arise from partial sequence complementary, and consequently, these aptamer pairs were eliminated from the study.

In search of the best-performing aptamer pair, the sensitivity of several combinations was then evaluated. Eight pairs were chosen based on both the specificity of the individual aptamers (Figure 2) and the relative binding they exhibited in the sandwich format (Figure 3). The pairs chosen were 1T/5B, 2T/1B, 3T/1B, 4T/1B, 5T/1B, 6T/6B, 1CT/6B, and 4CT/6B. S1 standard curves were thus constructed using the target protein in a range of 0.0032–50 μg/mL (equivalent to 0.042–654 nM), and the LODs were calculated as the bottoms of the curves fitted to the data using the four-parameter logistic model plus three times the standard deviation of the bottoms. As can be seen in Figure 4, high sensitivity was exhibited by all aptamer pairs tested, with LODs in the low nanomolar range (2.2–14.5 nM, equivalent to 0.17–1.11 μg/mL). EC50 values

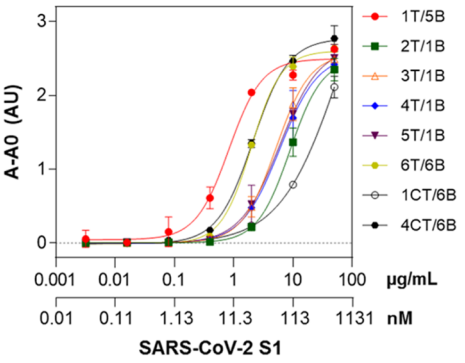

Aptamer pair	LOD		EC50		R^2
	µg/mL	nM	µg/mL	nM	
1T/5B	0.17	2.2	0.83	10.9	0.9882
2T/1B	1.11	14.5	8.90	116.3	0.9940
3T/1B	0.60	7.8	5.18	67.8	0.9947
4T/1B	0.72	9.4	6.02	78.7	0.9882
5T/1B	0.57	7.5	6.02	78.7	0.9914
6T/6B	0.27	3.5	1.98	25.9	0.9975
1CT/6B	0.44	5.7	66.84	873.7	0.9967
4CT/6B	0.21	2.7	2.12	27.7	0.9972

Figure 4. Sensitivity of the sandwich assays for SARS-CoV-2 S1 detection using different combinations of aptamer pairs.

https://doi.org/10.1021/acsomega.1c05521
ACS Omega 2021, 6, 35657–35666

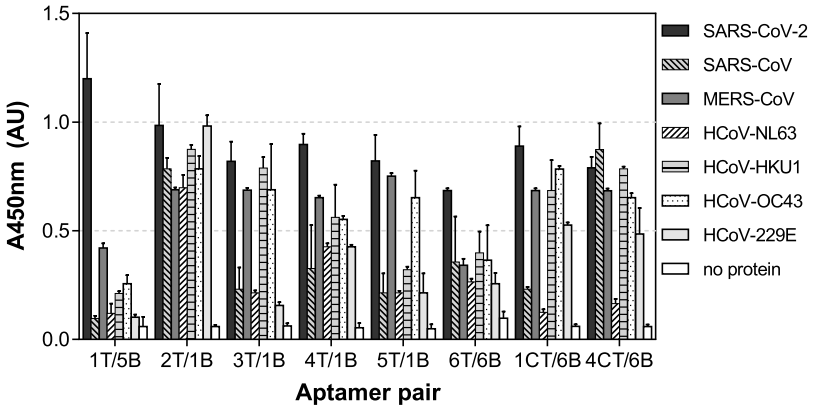

Figure 5. Specificity of the sandwich assays using different aptamer pairs and S1 from different HCoV's. Each protein was used at 2 μg/mL, and the error bars indicate the standard deviations from duplicate measurements.

varied from 10.9−873.7 nM (0.83−66.84 μg/mL). The best-performing pair was 1T/5B with an LOD of 2.2 nM (170 ng/mL) and an EC50 of 10.9 nM (830 ng/mL). It has to be pointed out that the assays were not optimized at this point; therefore, further improvement of their performance is expected following optimization.

In addition to sensitivity, specificity is one of the most important parameters defining the performance of an analytical assay. For this reason, the response of the sandwich assays to S1 domains from all known HCoV's was evaluated using the chosen aptamer pairs. As shown in Figure 5, the 1T/5B pair exhibited the highest specificity. The combination of Apt1 as a capture aptamer with Apt5 as a reporter aptamer decreased the cross-reactivity shown by the individual aptamers for HCoV-HKU1 and HCoV-OC43, confirming that sandwich formats can improve the specificity of analytical assays. However, some cross-reactivity with S1 from MERS-CoV was observed for the 1T/5B pair, similar to when the two aptamers were used individually. Cross-reactivity effects with MERS-CoV S-RBD protein were also observed with a near-infrared biosensor developed for SARS-CoV-2 S antigen detection using ACE2.[38] The same study also reported nonspecific signals from the SARS-CoV S protein and an influenza antigen. Since a cell membrane receptor was utilized as the biorecognition element, such interference from other viral antigens can be expected. In contrast, when specifically developed receptors such as aptamers and antibodies are used for bioassay design, cross-reactivity with other biomolecules can be prevented. Nevertheless, high antigen sequence and structural similarities can contribute to lower assay specificity even when monoclonal antibodies are used.[36] Consequently, the specificity exhibited by the 1T/5B pair was a decisive factor in choosing this pair for final assay development. The low cross-reactivity with the MERS-CoV antigen is not of critical importance since the occurrence of this virus in the population during the present pandemic is negligible.

Sensitivity of the Apt1T/Apt5B Pair for Sandwich Detection of SARS-CoV-2 S1. As mentioned earlier, an initial screening of the aptamer pairs was performed in order to choose the best-performing pair in terms of sensitivity and specificity. To improve the performance of the sandwich assay based on the 1T/5B aptamer pair, the concentrations of both capture (Apt1T) and reporter (Apt5B) aptamers were optimized. A checkerboard assay was carried out first using 31.25−2000 nM Apt1T aptamer in combination with 7.8−250 nM Apt5B aptamer. The highest signals were obtained for the 1T capture aptamer at concentrations ≥250 nM in combination with the Apt5B reporter aptamer at concentrations ≥125 nM (Figure S2, Supporting Information). The sensitivity of the assays was thus evaluated using 125−500 nM Apt5B reporter aptamer, while the capture aptamer Apt1T was maintained at the highest concentration tested (2000 nM). The lowest LODs were calculated when 125−250 nM Apt5B was used, enabling the detection of as low as 270−280 pM (21−22 ng/mL) S1 (Figure S3, Supporting Information). This corresponds to the improvement of 1 order of magnitude compared to when nonoptimized assay conditions were employed.

Since the final objective of the study is detection of the S antigen in NP swab samples from individuals suspected of having been infected with SARS-CoV-2, the compatibility of the assay with the viral transport media typically used to collect these samples was evaluated. Serial dilutions of the target S1 protein were prepared in viral transport medium (VTM), and the assay was performed as described earlier with some modifications. The volume of the sample or the standard protein analyzed was 25 μL. As can be observed in Figure 6, the performance of the assay under these modified conditions in VTM was similar to the one conducted under optimized conditions. The LOD was 190 pM (15 ng/mL) compared to 270 pM (21 ng/mL) calculated for the assay in PBS-based buffer. This corresponds to the detection of 375 pg of S1 in VTM, more than an order of magnitude lower than the sensitivity achieved by a rapid antigen test based on a sandwich between ACE2 and a spike protein monoclonal antibody (<5 ng of S1).[37] Recent reports exploiting the aptamers selected by Idili et al., in electrochemical aptamer-based (EAB) sensors, report detectability over a concentration range of 760 pg/mL−76 ng/mL[64] and detection limits of as low as ag/mL,[65] but real saliva or NP samples are not tested. Cennamo et al. also used Song's aptamers in a plasmonic D-shaped plastic optical fiber aptasensor, achieving a detection limit of 37 nM, but the sensor was not applied to the analysis of real samples.[66] Li et al. selected an aptamer against the wild-type and B.1.1.7 spike protein and demonstrated the use of the selected aptamers for the detection of a pseudotyped lentivirus in saliva samples, but again, no real samples from individuals with SARS-CoV-2 were analyzed.[51] In another work, the use of aptamer-functionalized gold nanoparticles was reported, achieving a detection limit of 10 nM, which is equivalent to 3540 genome copies/μL of

https://doi.org/10.1021/acsomega.1c05521
ACS Omega 2021, 6, 35657−35666

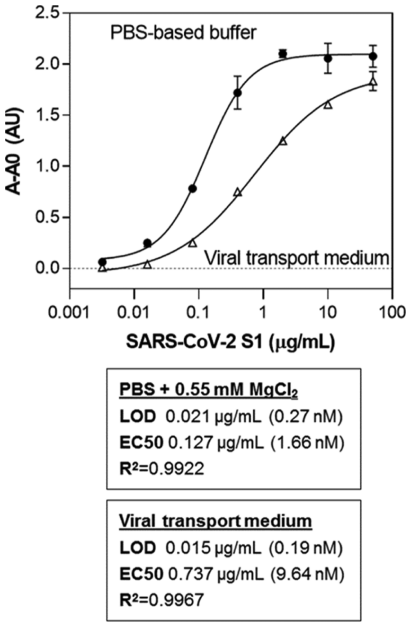

Figure 6. Sensitivity of the sandwich assay based on the Apt1T/Apt5B aptamer pair in aptamer binding buffer and in VTM.

inactivated SARS-CoV-2.[67] Using a 44-mer G-quadruplex-forming DNA aptamer they selected against the spike trimer antigen of SARS-CoV-2, Gupta et al. achieved a detection limit of 2 nM.[52] They used this aptamer for the analysis of 232 NP samples, achieving a highly discriminatory response between SARS-CoV-2-infected individuals from the noninfected ones with a sensitivity and specificity of 91 and 98%, respectively.[52]

The sensitivity of the assay compares well with other studies reported in the literature, exploiting antibodies or other biorecognition elements for the detection of the S antigen of SARS-CoV-2 (Table S3, Supporting Information). Overall, these results demonstrate the potential of aptamers for the sensitive detection of viral antigens even under non-native conditions such as VTM that would allow the analysis of clinical samples such as NP swab samples from suspected COVID-19 patients.

Application of the Assay to Clinical Samples. The assay was finally employed for the analysis of NP swab samples collected from individuals suspected of SARS-CoV-2 infection. Total RNA was extracted from these samples, and SARS-CoV-2 viral RNA was detected with droplet digital PCR (ddPCR), as described in the Supporting Information. Aptamer-based sandwich assay was performed as described in the previous section using VTM for the preparation of the standard curve samples. Ten negative samples (taken from individuals screened for COVID-19 and found not to have the infection) were analyzed, and the average signal obtained using these negative samples corresponded to 173 ng/mL, the highest signal obtained corresponded to 362 ng/mL, and 400 ng/mL was thus selected as the cutoff. Fifty samples taken from individuals who were confirmed to have the COVID-19 infection were analyzed. As can be seen in Table 2, the S1 antigen was detected in all positive samples, but applying the cutoff of 400 ng/mL established using the negative samples, nine false-negatives were obtained. Four false-positives were obtained, but these were samples taken from individuals who had been infected with COVID but in follow-up studies had then tested negative in PCR, and in these cases, there could still be some remaining antigen that was detected.

Table 2. Analysis of S1 in NP Swab Samples with the Aptamer Sandwich Assay and Comparison with PCR Results

test (target)	result	number of samples
PCR (viral RNA)	positive	45
	negative	5
aptamer sandwich assay (S antigen)	true positive	36
	false-positive	3
	true negative	1
	false-negative	9

CONCLUSIONS

Herein, we describe the characterization of RBD-binding aptamers for the development of a laboratory-based sandwich assay. The affinity of the aptamer candidates was evaluated, and K_D values in the low nanomolar range were obtained. The specificity of the aptamers was also studied using S1 from all seven known HCoV's, and Apt1 and Apt5 were observed to be the most specific aptamers, exhibiting only negligible cross-reactivity with the S1 from MERS-CoV. Using the Apt1 as a capture aptamer and the Apt5 as a reporter aptamer, an LOD of 21 ng/mL (270 pM) was obtained, corresponding to approximately 1 ng of S1 protein, while as low as 375 pg of S1 could be detected in VTM typically used for the collection of NP swab samples. NP swab samples from confirmed COVID-19 patients were analyzed, and the S antigen was detected in all positive samples, which had been previously verified by RT-ddPCR. However, applying the cutoff of 400 ng/mL established using the negative samples resulted in nine false-negatives. Work is ongoing to see if a component of the transport medium cross-reacts with the aptamers, resulting in this background signal, which would not be present if the swab was directly placed in a buffer, as would be the final format of the assay in a true application. In parallel, we are pursuing means to improve the assay sensitivity, combining with an antibody and also carrying out further truncation studies, and a higher number of real positive and negative samples need to be analyzed to elucidate true sensitivity and specificity values. To the best of our knowledge, this is the first report on the use of aptamers for the development of a SARS-CoV-2 antigen assay based on the S antigen. The work described herein is the first step toward the development of a rapid aptamer-based antigen test.

EXPERIMENTAL SECTION

Materials. Phosphate-buffered saline (PBS; 10 mM phosphate buffer, 137 mM NaCl, 2.7 mM KCl, pH 7.4), PBS-tween (PBS, 0.05% v/v Tween 20, pH 7.4), carbonate-bicarbonate buffer (50 mM, pH 9.4), MaxiSorp immunoassay plates, and maleimide-activated plates were purchased from Fisher Scientific (Madrid, Spain). Skim milk powder was from Merck (Barcelona, Spain), BioFX TMB super-sensitive one-component HRP microwell substrate was from Surmodics (USA), streptavidin-polyHRP80 (SA-polyHRP) was from Bionova Cientifica (Madrid, Spain), and VTM was from Vircell (Granada, Spain). Spike glycoprotein S1 proteins from the known HCoV's (SARS-CoV-2, SARS-CoV, MERS-CoV, HCoV-NL63, HCoV-HKU1, HCoV-OC43, and HCoV-229E, Table S1, Supporting Information) and the spike RBD from

https://doi.org/10.1021/acsomega.1c05521
ACS Omega 2021, 6, 35657−35666

SARS-CoV-2 were supplied from Sino Biological (Eschborn, Germany). The DNA aptamers,[46] with 5′-biotin or 5′-thiol-C6 modifications, were synthesized by Biomers.net (Ulm, Germany), and their sequences are shown in Table S2. The aptamer-binding buffer (BB) was composed of PBS containing 0.55 mM $MgCl_2$.

Evaluation of the Binding Properties of the Aptamers with a Direct Enzyme-Linked Aptamer Assay. The affinity and specificity of the aptamers were evaluated with a direct ELAA. For the affinity studies, SARS-CoV-2 spike S1 or RBD proteins (50 μL of 2 μg/mL in 50 mM carbonate buffer pH 9.4) were used to coat the wells of a 96-well plate, followed by blocking with 200 μL of 5% skimmed milk (w/v) in PBST. The wells were then incubated with 50 μL of serially diluted biotin-modified aptamers in binding buffer (200 nM down to 12.8 pM), followed by the addition of 50 μL of SA-polyHRP (50 ng/mL in PBST) for detection. Finally, 50 μL of the TMB substrate was added to each well and color development proceeded for 5 min at which point the reaction was stopped via the addition of an equal volume of 1 M sulfuric acid. The absorbance was read at 450 nm using a SpectraMax 340 PC microtiter plate reader. The affinity dissociation constants (K_D values) were determined by nonlinear regression analysis performed with the GraphPad Prism 6 software using the "one site-specific binding with Hill slope" model. For the specificity studies, S1 proteins from all seven known HCoV's (2 μg/mL each of SARS-CoV-2, SARS-CoV, MERS-CoV, HCoV-NL63, HCoV-HKU1, HCoV-229E, and HCoV-OC43) were immobilized on the plates and used in combination with 200 nM biotinylated aptamers as described above. All steps were performed for 30 min at ambient temperature (22−25 °C) under mild shaking conditions and the plates were washed (3 × 200 μL of PBST) between incubation steps. The relative binding (%) of the individual aptamers to each protein was calculated after normalization of the signals obtained to the responses for the target S1 protein from SARS-CoV-2. Data shown represent the mean ± SD from duplicate measurements and three independent experiments.

Screening of Aptamer Pairs for Sandwich ELAA Development. Sandwich-type ELAA assay was developed based on thiol-modified aptamers immobilized on maleimide-activated microtiter plate wells as capture aptamers in combination with biotinylated aptamers as reporters and SA-polyHRP for final detection. For screening of aptamer pairs and identification of aptamers forming a sandwich, each thiolated aptamer was used to coat the plate wells (50 μL of 500 nM in PBS) after overnight incubation at 4 °C. The plates were blocked with 200 μL of 5% skimmed milk (w/v) in PBST for 1 h at ambient temperature and then 50 μL of 2 μg/mL SARS-CoV-2 S1 protein in binding buffer were added to the wells. Following another 30 min incubation at ambient temperature and washing, the biotinylated aptamer (50 μL of 200 nM each in binding buffer) and SA-polyHRP (50 μL of 50 ng/mL in PBST) were added in sequential incubation steps followed by signal generation using TMB as described in the previous section. In total, 48 different aptamer combinations were evaluated for the detection of SARS-CoV-2 S1 in pairwise combinatorial experiments. The sensitivity of eight aptamer pairs was then studied. The pairs chosen were Apt1T/Apt5B, Apt2T/Apt1B, Apt3T/Apt1B, Apt4T/Apt1B, Apt5T/Apt1B, Apt6T/Apt6B, Apt1CT/Apt6B, and Apt4CT/Apt6B. Solutions of different concentrations of SARS-CoV-2 S1 protein were analyzed in the range of 42 pM−654 nM (equivalent to 3.2 ng/mL−50 μg/mL) using the conditions described above. The data were plotted using GraphPad Prism 6 software and fitted to a "Sigmoidal 4 parameter logistic" model. The LODs were interpolated from the fitted curves as the bottom of the curves plus three times the standard deviation of the bottom. The specificity of the same aptamer combinations was finally assessed using S1 proteins (2 μg/mL each in binding buffer) from all seven HCoV's as described above. The data represent the mean ± SD from duplicate measurements and three independent experiments.

Optimization of Sandwich Assay Conditions for S1 Detection with the Apt1T/Apt5B Aptamer Pair. A checkerboard titration experiment was initially performed, varying the concentrations of both capture (Apt1T) and detection (Apt5B) aptamers, to optimize their concentrations at a constant SARS-CoV-2 S1 protein concentration (2 μg/mL). Apt1T starting solution of 2000 nM was serially diluted twofold down to 31.3 nM, whereas Apt5B was used in the range of 250 nM down to 7.8 nM. Next, the performance of the assay was evaluated to elucidate the LOD and EC50 using the Apt1T at the maximum concentration (2000 nM) to coat the maleimide-activated plate and the Apt5B at 125, 250, and 500 nM. S1 protein was analyzed in the range of 50 μg/mL down to 3.2 ng/mL using 50 μL per well, as detailed in the previous section.

Detection of the S Antigen in NP Swab Samples. The sandwich aptamer assay with the Apt1T/Apt5B aptamer pair was finally employed to analyze NP swab samples from the COVID-19 Cohort of the Galicia Sur Health Research Institute (COHVID-GS) (https://www.iisgaliciasur.es/apoyo-a-la-investigacion/cohorte-covid19/) including samples from individuals with a confirmed diagnosis of COVID-19 (n = 50) and healthy donors (n = 10). The specimens were collected in VTM, and ddPCR was performed to verify the presence of viral RNA in the samples, as detailed in the Supporting Information The samples were heated for 30 min at 65 °C to deactivate any remaining viral particles and used without dilution for analysis, as explained in the previous sections with some modifications. Specifically, 500 nM Apt1T capture aptamer was immobilized on the wells of the maleimide-activated plate, the volume of the sample or the standard protein was 25 μL instead of 50 μL, the sample incubation step was 1 h instead of 30 min, and the Apt5B reporter aptamer was used at 150 nM. The S1 protein standard calibration curve was constructed in parallel in VTM to facilitate the quantification of the antigen level in the samples. Each sample was analyzed in duplicate and the average signals obtained for each sample in wells with and without the Apt1T aptamer were used to interpolate the S1 antigen concentration from the calibration curve.

■ ASSOCIATED CONTENT

Supporting Information

The Supporting Information is available free of charge at https://pubs.acs.org/doi/10.1021/acsomega.1c05521.

Recombinant proteins and aptamers used in this work; biosensors and assays developed for the detection of the SARS-CoV-2 S antigen; binding studies by direct ELAA to monitor S proteins interactions with aptamers; checkerboard titration of concentrations of capture and detection aptamers to optimize aptamer sandwich assay; sensitivity of the sandwich aptamer assay at different

https://doi.org/10.1021/acsomega.1c05521
ACS Omega 2021, 6, 35657−35666

concentrations of reporter aptamer; and SARS-CoV-2 RNA detection in NP swab samples by droplet digital PCR analysis (PDF)

AUTHOR INFORMATION

Corresponding Author

Ciara K. O'Sullivan − *INTERFIBIO Research Group, Departament d'Enginyeria Química, Universitat Rovira i Virgili, Tarragona 43007, Spain; Institució Catalana de Recerca i Estudis Avancats (ICREA), Barcelona 08010, Spain;* orcid.org/0000-0003-2603-2230; Email: ciara.osullivan@urv.cat

Authors

Marketa Svobodova − *INTERFIBIO Research Group, Departament d'Enginyeria Química, Universitat Rovira i Virgili, Tarragona 43007, Spain*

Vasso Skouridou − *INTERFIBIO Research Group, Departament d'Enginyeria Química, Universitat Rovira i Virgili, Tarragona 43007, Spain;* orcid.org/0000-0002-9712-5429

Miriam Jauset-Rubio − *INTERFIBIO Research Group, Departament d'Enginyeria Química, Universitat Rovira i Virgili, Tarragona 43007, Spain*

Irene Viéitez − *Rare Diseases & Pediatric Medicine Research Group, Galicia Sur Health Research Institute (IIS Galicia Sur), SERGAS-Uvigo, Vigo 36213, Spain;* orcid.org/0000-0001-9241-0207

Alberto Fernández-Villar − *Pneumology Service, Galicia Sur Health Research Institute (IIS Galicia Sur), SERGAS-Uvigo, Vigo 36213, Spain*

Jorge Julio Cabrera Alvargonzalez − *Microbiology Service, Galicia Sur Health Research Institute (IIS Galicia Sur). SERGAS-UVigo, Vigo 36213, Spain*

Eva Poveda − *Group of Virology and Pathogenesis, Galicia Sur Health Research Institute (IIS Galicia Sur)-Complexo Hospitalario Universitario de Vigo, SERGAS-UVigo, Vigo 36213, Spain*

Clara Benavent Bofill − *Laboratori Clinic ICS Camp de Tarragona, Hospital Universitari de Tarragona Joan XXIII, Tarragona 43007, Spain*

Teresa Sans − *Laboratori Clinic ICS Camp de Tarragona, Hospital Universitari de Tarragona Joan XXIII, Tarragona 43007, Spain*

Abdulaziz Bashammakh − *Department of Chemistry, Faculty of Science, King Abdulaziz University, Jeddah 80215, Kingdom of Saudi Arabia*

Abdulrahman O. Alyoubi − *Department of Chemistry, Faculty of Science, King Abdulaziz University, Jeddah 80215, Kingdom of Saudi Arabia*

Complete contact information is available at: https://pubs.acs.org/10.1021/acsomega.1c05521

Author Contributions

○M.S. and V.S. contributed equally.

Funding

The COHVID-GS is funded by Fondo COVID-19 of Instituto de Salud Carlos III (COV20/00698) and Fundación Biomédica Galicia Sur. King Abdulaziz University has contributed to the funding of this work.

Notes

The authors declare no competing financial interest.

♦On behalf of the Cohort COVID-19 of the Galicia Sur Health Research Institute.

ACKNOWLEDGMENTS

We would like to thank all the members of COHVID-GS and IISGS Biobank. Members of COHVID-GS (Galicia Sur Health Research Institute): Alejandro Araujo, Jorge Julio Cabrera, Víctor del Campo, Manuel Crespo, Alberto Fernández, Beatriz Gil de Araujo, Carlos Gómez, Virginia Leiro, María Rebeca Longueira, Ana López-Domínguez, José Ramón Lorenzo, María Marcos, Alexandre Pérez, María Teresa Pérez, Lucia Patiño, Sonia Pérez, Silvia Pérez-Fernández, E.P., Cristina Ramos, Benito Regueiro, Cristina Retresas, Tania Rivera, Olga Souto, Isabel Taboada, Susana Teijeira, María Torres, Vanesa Val, and I.V.é

REFERENCES

(1) Weiss, S. R. Forty years with coronaviruses. *J. Exp. Med.* **2020**, *217*, No. e20200537.

(2) He, F.; Deng, Y.; Li, W. Coronavirus disease 2019: What we know? *J. Med. Virol.* **2020**, *92*, 719−725.

(3) Zhu, Z.; Lian, X.; Su, X.; Wu, W.; Marraro, G. A.; Zeng, Y. From SARS and MERS to COVID-19: a brief summary and comparison of severe acute respiratory infections caused by three highly pathogenic human coronaviruses. *Respir. Res.* **2020**, *21*, 224.

(4) Gorbalenya, A. E.; Baker, S. C.; Baric, R. S.; de Groot, R. J.; Drosten, C.; Gulyaeva, A. A.; Haagmans, B. L.; Lauber, C.; Leontovich, A. M.; Neuman, B. W.; Penzar, D.; Perlman, S.; Poon, L. L. M.; Samborskiy, D. V.; Sidorov, I. A.; Sola, I.; Ziebuhr, J. The species Severe Acute Respiratory Syndrome-related coronavirus: classifying 2019-nCoV and naming it SARS-CoV-2. *Nat. Microbiol.* **2020**, *5*, 536−544.

(5) Wrapp, D.; Wang, N.; Corbett, K. S.; Goldsmith, J. A.; Hsieh, C.-L.; Abiona, O.; Graham, B. S.; McLellan, J. S. Cryo-EM structure of the 2019-nCoV spike in the prefusion conformation. *Science* **2020**, *367*, 1260−1263.

(6) Wang, N.; Shang, J.; Jiang, S.; Du, L. Subunit vaccines against emerging pathogenic human coronaviruses. *Front. Microbiol.* **2020**, *11*, 298.

(7) Yao, H.; Song, Y.; Chen, Y.; Wu, N.; Xu, J.; Sun, C.; Zhang, J.; Weng, T.; Zhang, Z.; Wu, Z.; Cheng, L.; Shi, D.; Lu, X.; Lei, J.; Crispin, M.; Shi, Y.; Li, L.; Li, S. Molecular architecture of the SARS-CoV-2 virus. *Cell* **2020**, *183*, 730−738 e13.

(8) Zhou, Y.; Jiang, S.; Du, L. Prospects for a MERS-CoV spike vaccine. *Expert Rev. Vaccines* **2018**, *17*, 677−686.

(9) Lan, J.; Ge, J.; Yu, J.; Shan, S.; Zhou, H.; Fan, S.; Zhang, Q.; Shi, X.; Wang, Q.; Zhang, L.; Wang, X. Structure of the SARS-CoV-2 spike receptor-binding domain bound to the ACE2 receptor. *Nature* **2020**, *581*, 215−220.

(10) Li, F.; Li, W.; Farzan, M.; Harrison, S. C. Structure of SARS coronavirus spike receptor-binding domain complexed with receptor. *Science* **2005**, *309*, 1864−1868.

(11) Liu, S.; Xiao, G.; Chen, Y.; He, Y.; Niu, J.; Escalante, C. R.; Xiong, H.; Farmar, J.; Debnath, A. K.; Tien, P.; Jiang, S. Interaction between heptad repeat 1 and 2 regions in spike protein of SARS-associated coronavirus: implications for virus fusogenic mechanism and identification of fusion inhibitors. *Lancet* **2004**, *363*, 938−947.

(12) Tai, W.; He, L.; Zhang, X.; Pu, J.; Voronin, D.; Jiang, S.; Zhou, Y.; Du, L. Characterization of the receptor-binding domain (RBD) of 2019 novel coronavirus: implication for development of RBD protein as a viral attachment inhibitor and vaccine. *Cell. Mol. Immunol.* **2020**, *17*, 613−620.

(13) Dai, L.; Gao, G. F. Viral targets for vaccines against COVID-19. *Nat. Rev. Immunol.* **2021**, *21*, 73−82.

(14) Khan, S.; Tombuloglu, H.; Hassanein, S. E.; Rehman, S.; Bozkurt, A.; Cevik, E.; Abdel-Ghany, S.; Nabi, G.; Ali, A.; Sabit, H.

Coronavirus diseases 2019: current biological situation and potential therapeutic perspective. *Eur. J. Pharmacol.* **2020**, *886*, 1733447.
(15) Tombuloglu, H.; Sabit, H.; Al-Suhaimi, E.; Al Jindan, R.; Alkharsah, K. R. Development of multiplex real-time RT-PCR assay for the detection of SARS-CoV-2. *PLoS One* **2021**, *16*, No. e0250942.
(16) Ravi, N.; Cortade, D. L.; Ng, E.; Wang, S. X. Diagnostics for SARS-CoV-2 detection: a comprehensive review of the FDA-EUA COVID-19 testing landscape. *Biosens. Bioelectron.* **2020**, *165*, 112454.
(17) Abbott Diagnostics Scarborough Inc. *BinaxNOWTM COVID-19 Ag CARD [package insert, EUA]*; Scarborough: MA, USA, 2020.
(18) LumiraDx Group Limited. *LumiraDxTM SARS-CoV-2 Ag Test [package insert, EUA]*; Dumyat Business Park Alloa FK10 2PB: U.K., 2020.
(19) Becton, Dickinson and Company. *BD VeritorTM System for Rapid Detection of SARS-CoV-2 [package insert, EUA]*; Sparks-Glencoe: MD, USA, 2020.
(20) Quidel Corporation. *Sofia Severe Acute Respiratory Syndrome Antigen FIA [package insert, EUA]*: San Diego, CA, USA, 2020.
(21) Barlev-Gross, M.; Weiss, S.; Ben-Shmuel, A.; Sittner, A.; Eden, K.; Mazuz, N.; Glinert, I.; Bar-David, E.; Puni, R.; Amit, S.; Kriger, O.; Schuster, O.; Alcalay, R.; Makdasi, E.; Epstein, E.; Noy-Porat, T.; Rosenfeld, R.; Achdout, H.; Mazor, O.; Israely, T.; Levy, H.; Mechaly, A. Spike vs nucleocapsid SARS-CoV-2 antigen detection: application in nasopharyngeal swab specimens. *Anal. Bioanal. Chem.* **2021**, *413*, 3501−3510.
(22) Aoki, K.; Nagasawa, T.; Ishii, Y.; Yagi, S.; Okuma, S.; Kashiwagi, K.; Maeda, T.; Miyazaki, T.; Yoshizawa, S.; Tateda, K. Clinical validation of quantitative SARS-CoV-2 antigen assays to estimate SARS-CoV-2 viral loads in nasopharyngeal swabs. *J. Infect. Chemother.* **2021**, *27*, 613−616.
(23) Hirotsu, Y.; Maejima, M.; Shibusawa, M.; Nagakubo, Y.; Hosaka, K.; Amemiya, K.; Sueki, H.; Hayakawa, M.; Mochizuki, H.; Tsutsui, T.; Kakizaki, Y.; Miyashita, Y.; Yagi, S.; Kojima, S.; Omata, M. Comparison of automated SARS-CoV-2 antigen test for COVID-19 infection with quantitative RT-PCR using 313 nasopharyngeal swabs, including from seven serially followed patients. *Int. J. Infect. Dis.* **2020**, *99*, 397−402.
(24) Pollock, N. R.; Savage, T. J.; Wardell, H.; Lee, R.; Mathew, A.; Stengelin, M.; Sigal, G. B. Correlation of SARS-CoV-2 nucleocapsid antigen and RNA concentrations in nasopharyngeal samples from children and adults using an ultrasensitive and quantitative antigen assay. *J. Clin. Microbiol.* **2021**, *59*, e03077−20.
(25) Pekosz, A.; Cooper, C. K.; Parvu, V.; Li, M.; Andrews, J. C.; Manabe, Y. C.; Kodsi, S.; Leitch, J.; Gary, D. S.; Roger-Dalbert, C. Antigen-based testing but not real-time polymerase chain reaction correlates with Severe Acute Respiratory Syndrome Coronavirus 2 viral culture. *Clin. Infect. Dis.* **2021**, *73*, e2861−e2866.
(26) Scohy, A.; Anantharajah, A.; Bodéus, M.; Kabamba-Mukadi, B.; Verroken, A.; Rodriguez-Villalobos, H. Low performance of rapid antigen detection test as frontline testing for COVID-19 diagnosis. *J. Clin. Virol.* **2020**, *129*, 104455.
(27) Tang, Y. W.; Schmitz, J. E.; Persing, D. H.; Stratton, C. W. Laboratory diagnosis of COVID-19: current issues and challenges. *J. Clin. Microbiol.* **2020**, *58*, 10−1128.
(28) Che, X.-y.; Qiu, L.-w.; Pan, Y.-x.; Wen, K.; Hao, W.; Zhang, L.-y.; Wang, Y.-d.; Liao, Z.-y.; Hua, X.; Cheng, V. C. C.; Yuen, K.-y. Sensitive and specific monoclonal antibody-based capture enzyme immunoassay for detection of nucleocapsid antigen in sera from patients with Severe Acute Respiratory Syndrome. *J. Clin. Microbiol.* **2004**, *42*, 2629−2635.
(29) Diao, B.; Wen, K.; Chen, J.; Liu, Y.; Yuan, Z.; Han, C.; Chen, J.; Pan, Y.; Chen, L.; Dan, Y.; Wang, J.; Chen, Y.; Deng, G.; Zhou, H.; Wu, Y. Diagnosis of acute respiratory syndrome coronavirus 2 infection by detection of nucleocapsid protein. *medRxiv* **2020**, 20032524.
(30) Grant, B. D.; Anderson, C. E.; Williford, J. R.; Alonzo, L. F.; Glukhova, V. A.; Boyle, D. S.; Weigl, B. H.; Nichols, K. P. SARS-CoV-2 coronavirus nucleocapsid antigen-detecting half-strip lateral flow assay toward the development of point of care tests using commercially available reagents. *Anal. Chem.* **2020**, *92*, 11305−11309.
(31) Ahmadivand, A.; Gerislioglu, B.; Ramezani, Z.; Kaushik, A.; Manickam, P.; Ghoreishi, S. A. Functionalized terahertz plasmonic metasensors: femtomolar-level detection of SARS-CoV-2 spike proteins. *Biosens. Bioelectron.* **2021**, *177*, 112971.
(32) Seo, G.; Lee, G.; Kim, M. J.; Baek, S.-H.; Choi, M.; Ku, K. B.; Lee, C.-S.; Jun, S.; Park, D.; Kim, H. G.; Kim, S.-J.; Lee, J.-O.; Kim, B. T.; Park, E. C.; Kim, S. I. Rapid detection of COVID-19 causative virus (SARS-CoV-2) in human nasopharyngeal swab specimens using field-effect transistor-based biosensor. *ACS Nano* **2020**, *14*, 5135−5142.
(33) Zhong, J.; Rösch, E. L.; Viereck, T.; Schilling, M.; Ludwig, F. Toward rapid and sensitive detection of SARS-CoV-2 with functionalized magnetic nanoparticles. *ACS Sens.* **2021**, *6*, 976−984.
(34) Ventura, B. D.; Cennamo, M.; Minopoli, A.; Campanile, R.; Censi, S. B.; Terracciano, D.; Portella, G.; Velotta, R. Colorimetric test for fast detection of SARS-CoV-2 in nasal and throat swabs. *ACS Sens.* **2020**, *5*, 3043−3048.
(35) Pramanik, A.; Gao, Y.; Patibandla, S.; Mitra, D.; McCandless, M. G.; Fassero, L. A.; Gates, K.; Tandon, R.; Chandra Ray, P. The rapid diagnosis and effective inhibition of coronavirus using spike antibody attached gold nanoparticles. *Nanoscale Adv.* **2021**, *3*, 1588−1596.
(36) Yousefi, H.; Mahmud, A.; Chang, D.; Das, J.; Gomis, S.; Chen, J. B.; Wang, H.; Been, T.; Yip, L.; Coomes, E.; Li, Z.; Mubareka, S.; McGeer, A.; Christie, N.; Gray-Owen, S.; Cochrane, A.; Rini, J. M.; Sargent, E. H.; Kelley, S. O. Detection of SARS-CoV-2 viral particles using direct, reagent-free electrochemical sensing. *J. Am. Chem. Soc.* **2021**, *143*, 1722−1727.
(37) Lee, J.-H.; Choi, M.; Jung, Y.; Lee, S. K.; Lee, C.-S.; Kim, J.; Kim, J.; Kim, N. H.; Kim, B.-T.; Kim, H. G. A novel rapid detection for SARS-CoV-2 spike 1 antigens using human angiotensin converting enzyme 2 (ACE2). *Biosens. Bioelectron.* **2021**, *171*, 112715.
(38) Pinals, R. L.; Ledesma, F.; Yang, D.; Navarro, N.; Jeong, S.; Pak, J. E.; Kuo, L.; Chuang, Y.-C.; Cheng, Y.-W.; Sun, H.-Y.; Landry, M. P. Rapid SARS-CoV-2 spike protein detection by carbon nanotube-based near-infrared nanosensors. *Nano Lett.* **2021**, *21*, 2272−2280.
(39) Baker, A. N.; Richards, S.-J.; Guy, C. S.; Congdon, T. R.; Hasan, M.; Zwetsloot, A. J.; Gallo, A.; Lewandowski, J. R.; Stansfeld, P. J.; Straube, A.; Walker, M.; Chessa, S.; Pergolizzi, G.; Dedola, S.; Field, R. A.; Gibson, M. I. The SARS-COV-2 spike protein binds sialic acids and enables rapid detection in a lateral flow point of care diagnostic device. *ACS Cent. Sci.* **2020**, *6*, 2046−2052.
(40) Tuerk, C.; Gold, L. Systematic evolution of ligands by exponential enrichment: RNA ligands to bacteriophage T4 DNA polymerase. *Science* **1990**, *249*, 505−510.
(41) Ellington, A. D.; Szostak, J. W. In vitro selection of RNA molecules that bind specific ligands. *Nature* **1990**, *346*, 818−822.
(42) Robertson, D. L.; Joyce, G. F. Selection in vitro of an RNA enzyme that specifically cleaves single-stranded DNA. *Nature* **1990**, *344*, 467−468.
(43) Nguyen, V.-T.; Seo, H. B.; Kim, B. C.; Kim, S. K.; Song, C.-S.; Gu, M. B. Highly sensitive sandwich-type SPR based detection of whole H5Nx viruses using a pair of aptamers. *Biosens. Bioelectron.* **2016**, *86*, 293−300.
(44) Park, J.-W.; Jin Lee, S.; Choi, E.-J.; Kim, J.; Song, J.-Y.; Bock Gu, M. An ultra-sensitive detection of a whole virus using dual aptamers developed by immobilization-free screening. *Biosens. Bioelectron.* **2014**, *51*, 324−329.
(45) Seo, H. B.; Gu, M. B. Aptamer-based sandwich-type biosensors. *J. Biol. Eng.* **2017**, *11*, 11.
(46) Song, Y.; Song, J.; Wei, X.; Huang, M.; Sun, M.; Zhu, L.; Lin, B.; Shen, H.; Zhu, Z.; Yang, C. Discovery of aptamers targeting the receptor-binding domain of the SARS-CoV-2 spike glycoprotein. *Anal. Chem.* **2020**, *92*, 9895−9900.
(47) Stanborough, T.; Given, F. M.; Koch, B.; Sheen, C. R.; Stowers-Hull, A. B.; Waterland, M. R.; Crittenden, D. L. Optical detection of

https://doi.org/10.1021/acsomega.1c05521
ACS Omega 2021, 6, 35657−35666

CoV-SARS-2 viral proteins to sub-picomolar concentrations. *ACS Omega* **2021**, *6*, 6404−6413.
(48) Pramanik, A.; Gao, Y.; Patibandla, S.; Mitra, D.; McCandless, M. G.; Fassero, L. A.; Gates, K.; Tandon, R.; Ray, P. C. Aptamer conjugated gold nanostar-based distance-dependent nanoparticle surface energy transfer spectroscopy for ultrasensitive detection and inactivation of corona virus. *J. Phys. Chem. Lett.* **2021**, *12*, 2166−2171.
(49) Schmitz, A.; Weber, A.; Bayin, M.; Breuers, S.; Fieberg, V.; Famulok, M.; Mayer, G. A SARS-CoV-2 spike binding DNA aptamer that inhibits pseudovirus infection by an RBD-independent mechanism. *Angew. Chem., Int. Ed.* **2021**, *60*, 2−9.
(50) Yang, G.; Li, Z.; Mohammed, I.; Zhao, L.; Wei, W.; Xiao, H.; Guo, W.; Zhao, Y.; Qu, F.; Huang, Y. Identification of SARS-CoV-2-against aptamer with high neutralization activity by blocking the RBD domain of spike protein 1. *Signal Transduction Targeted Ther.* **2021**, *6*, 227.
(51) Li, J.; Zhang, Z.; Gu, J.; Stacey, H. D.; Ang, J. C.; Capretta, A.; Filipe, C. D. M.; Mossman, K. L.; Balion, C.; Salena, B. J.; Yamamura, D.; Soleymani, L.; Miller, M. S.; Brennan, J. D.; Li, Y. Diverse high-affinity DNA aptamers for wild-type and B.1.1.7 SARS-CoV-2 spike proteins from a pre-structured DNA library. *Nucleic Acids Res.* **2021**, *49*, 7267−7279.
(52) Gupta, A.; Anand, A.; Jain, N.; Goswami, S.; Anantharaj, A.; Patil, S.; Singh, R.; Kumar, A.; Shrivastava, T.; Bhatnagar, S.; Medigeshi, G. R.; Sharma, T. K.; DBT India Consortium for COVID-19 Research. A novel G-quadruplex aptamer-based spike trimeric antigen test for the detection of SARS-CoV-2. *Mol. Ther.–Nucleic Acids* **2021**, *26*, 321−332.
(53) Alves Ferreira-Bravo, I.; DeStefano, J. J. Xeno-nucleic Acid (XNA) 2'-fluoro-arabino nucleic acid (FANA) aptamers to the receptor-binding domain of SARS-CoV-2 S protein block ACE2 binding. *Viruses* **2021**, *13*, 1983.
(54) Behbahani, M.; Mohabatkar, H.; Hosseini, B. In silico design of quadruplex aptamers against the spike protein of SARS-CoV-2. *Inf. Med.* **2021**, *26*, 100757.
(55) Devi, A.; Chaitanya, N. S. N. Designing of peptide aptamer targeting the receptor-binding domain of spike protein of SARS-CoV-2: an in silico study. *Mol. Diversity* **2021**, 1−13.
(56) Artyushenko, P. V.; Mironov, V. A.; Mironov, V. A.; Morozov, D. I.; Shchugoreva, I. A.; Borbone, N.; Tomilin, F. N.; Kichkailo, A. S. Computational approach to design of aptamers to the receptor binding domain of SARS-CoV-2. *Sib. Med. Rev.* **2021**, *2*, 66−67.
(57) Kowada, A. Greater public health impact of COVID-19 antigen detection tests. *BMC Med.* **2021**, *19*, 82.
(58) Pomplun, S.; Jbara, M.; Quartararo, A. J.; Zhang, G.; Brown, J. S.; Lee, Y.-C.; Ye, X.; Hanna, S.; Pentelute, B. L. De novo discovery of high-affinity peptide binders for the SARS-CoV-2 spike protein. *ACS Cent. Sci.* **2021**, *7*, 156−163.
(59) Kaur, N.; Singh, R.; Dar, Z.; Bijarnia, R. K.; Dhingra, N.; Kaur, T. Genetic comparison among various coronavirus strains for the identification of potential vaccine targets of SARS-CoV2. *Infect., Genet. Evol.* **2021**, *89*, 104490.
(60) Loos, C.; Atyeo, C.; Fischinger, S.; Burke, J.; Slein, M. D.; Streeck, H.; Lauffenburger, D.; Ryan, E. T.; Charles, R. C.; Alter, G. Evolution of early SARS-CoV-2 and cross-coronavirus immunity. *mSphere* **2020**, *5*, e00622−20.
(61) Li, F. Structure, function, and evolution of coronavirus spike proteins. *Annu. Rev. Virol.* **2016**, *3*, 237−261.
(62) Andersen, K. G.; Rambaut, A.; Lipkin, W. I.; Holmes, E. C.; Garry, R. F. The proximal origin of SARS-CoV-2. *Nat. Med.* **2020**, *26*, 450−452.
(63) Ou, X.; Liu, Y.; Lei, X.; Li, P.; Mi, D.; Ren, L.; Guo, L.; Guo, R.; Chen, T.; Hu, J.; Xiang, Z.; Mu, Z.; Chen, X.; Chen, J.; Hu, K.; Jin, Q.; Wang, J.; Qian, Z. Characterization of spike glycoprotein of SARS-CoV-2 on virus entry and its immune cross-reactivity with SARS-CoV. *Nat. Commun.* **2020**, *11*, 1620.
(64) Idili, A.; Parolo, C.; Alvarez-Diduk, R.; Merkoçi, A. Rapid and efficient detection of the SARS-CoV-2 spike protein using an electrochemical aptamer-based sensor. *ACS Sens.* **2021**, *6*, 3093−3101.
(65) Zakashansky, J. A.; Imamura, A. H.; Salgado, D. F., 2nd; Romero Mercieca, H. C.; Aguas, R. F. L.; Lao, A. M.; Pariser, J.; Arroyo-Currás, N.; Khine, M. Detection of the SARS-CoV-2 spike protein in saliva with Shrinky-Dink electrodes. *Anal. Methods* **2021**, *13*, 874−883.
(66) Cennamo, N.; Pasquardini, L.; Arcadio, F.; Lunelli, L.; Vanzetti, L.; Carafa, V.; Altucci, L.; Zeni, L. SARS-CoV-2 spike protein detection through a plasmonic D-shaped plastic optical fiber aptasensor. *Talanta* **2021**, *233*, 122532.
(67) Aithal, S.; Mishriki, S.; Gupta, R.; Sahu, R. P.; Botos, G.; Tanvir, S.; Hanson, R. W.; Puri, I. K. SARS-CoV-2 detection with aptamer-functionalized gold nanoparticles. *Talanta* **2022**, *236*, 122841.

https://doi.org/10.1021/acsomega.1c05521
ACS Omega 2021, 6, 35657−35666